ELSEVIER

Biophysical Chemistry 94 (2001) 87–96

Biophysical Chemistry

www.elsevier.com/locate/bpc

Studies on the size and stability of chlorpromazine hydrochloride nanostructures in aqueous solution

Shandiz Tehrani, Nathan Brandstater, Yoshihito David Saito, Phoebe Dea*

Department of Chemistry, Occidental College, Los Angeles, CA 90041, USA

Received 18 July 2001; received in revised form 31 August 2001; accepted 31 August 2001

Abstract

The mean aggregate number (MAN) of the antipsychotic drug chlorpromazine hydrochloride (CPZ) nanostructure was investigated by fluorescence quenching using 9-methylanthracene (9-MA) as the quencher. The method was designed to take advantage of the intrinsic fluorescent properties of CPZ. The validity of this method was supported by the results obtained for the MAN which was determined to be approximately 37 for a solution of 10 mM CPZ in 0.1 M pH 6.5 phosphate buffer. An increase in the aggregate size with increasing drug concentration confirmed the stepwise aggregation theory of CPZ micelle formation. Differential scanning calorimetry was used to examine the effects of concentration on the thermodynamics of micellization. The enthalpy of demicellization increased with increasing CPZ concentration (5–12 mM), suggesting a greater stability of the aggregates at higher concentrations. At amphiphile concentrations higher than 12 mM, a plateau of approximately 10 kJ/mol was observed as the enthalpy of demicellization. Fluorescence lifetime results revealed a two-component system at low CPZ concentration, while data at amphiphile concentrations higher than 12 mM could not be fitted to either single or multi-component lifetime values, suggesting an increase in dispersity in these nanostructures at higher CPZ concentrations. Temperatures higher than 40°C tend to destabilize the larger micelles, and demicellization was observed after approximately 45°C. Changes in osmotic pressure in the presence of dextrose up to 0.3 M had no significant effect on the size of these micellar nanostructures. © 2001 Elsevier Science B.V. All rights reserved.

Keywords: Chlorpromazine; Nanostructures; Micellization; Thermodynamics; Fluorescence; DSC

Abbreviations: CPZ, chlorpromazine hydrochloride; 9-MA, 9-methylanthracene; MAN, mean aggregate number; DSC, differential scanning calorimetry

* Corresponding author. Tel.: +1-323-259-2625; fax: +1-323-341-4912.
E-mail address: dea@oxy.edu (P. Dea).

0301-4622/01/$ - see front matter © 2001 Elsevier Science B.V. All rights reserved.
PII: S0301-4622(01)00226-5

1. Introduction

The importance and widespread use of the phenothiazine tranquilizers in the treatment of psychotic disorders is well known [1]. Yet, despite numerous studies [2–6], the precise mechanism of biological interaction is unknown. The pharmacological activity of phenothiazines is in general concentration-dependent, and the effects on the physical properties of membranes differ at low and high concentrations [7]. The heterocyclic, lipophilic portion of chlorpromazine hydrochloride (CPZ) is characteristic of all members of the phenothiazine group. Chlorpromazine forms micellar systems of nanostructures that undergo concentration, temperature, and pH-dependent phase transitions [8–10]. Binding results for the interaction of CPZ with brain tubulin reveal preferential binding of the micellar state of the drug [11–13]. The understanding of CPZ monomer and micelle behaviors as a function of concentration and temperature is therefore critical for the elucidation of the drug's pharmacological and biochemical mechanism of action.

The structure of the CPZ monomer reveals a protonated tertiary amine moiety, which results in the amphiphilic character of the drug. Aggregation of the monomers at and above the critical micelle concentration (cmc) is governed by the hydrophobic effect [14], and stabilized by the $\pi-\pi$ stacking of the aromatic rings [15,16]. The self-association of CPZ results in a thermodynamically stabilized supramolecular nanostructure, in which the interaction between lipophilic aromatic rings and polar solvent molecules are reduced [9]. The CPZ aggregate size depends on a number of parameters, as discovered by previous methods including gel filtration chromatography [8], light scattering [17,18], small-angle neutron scattering [19], and sedimentation equilibrium [20].

The method of fluorescence quenching has been widely used to study the aggregation behavior of non-fluorescent amphiphilic molecules [21–23], following the work carried out by Turro and Yekta on sodium dodecyl sulfate [21]. The approach involves the measurement of steady-state fluorescence of a hydrophobic probe molecule as a function of a non-polar quencher concentration. Here we report results obtained using a modified version of the quenching method, in which the intrinsic fluorescent properties of the analyte eliminates the need for a fluorescent probe. The underlying assumptions in the quenching method are closely approximated. In addition, the thermodynamics of demicellization were studied using differential scanning calorimetry and measurements of fluorescence lifetimes added to our understanding of the polydispersity of these micellar nanostructures.

2. Materials and methods

2.1. Chemicals and instrumentation

Chlorpromazine hydrochloride (ICN Biomedicals, Aurora, OH, 98 + %) and 9-methylanthracene (Aldrich, Milwaukee, WI 98%) were used without further purification. Analytical grade sodium chloride, dextrose, and monobasic and dibasic sodium phosphate were purchased from J.T. Baker. All stock solutions were prepared using water purified with the Millipore Milli-Q Plus water purifier (Bedford, MA), and reagent grade ethanol. Steady-state fluorescence and lifetimes were measured with an ISS K2 multifrequency cross-correlation phase and modulation fluorometer with a xenon arc lamp (Champaign, IL), and thermally equilibrated by a Neslab RTE 111 bath (Portsmouth, NH). A 1-cm quartz cuvette was used in fluorescence acquisition. Differential scanning calorimeter scans were made using a Calorimetry Sciences, Inc. multi-cell DSC H-T model 4100.

2.2. Sample preparation

Nitrogen-saturated 0.1 M phosphate buffer (pH 6.3) was used to prepare 0.1 M stock solutions of CPZ. The solutions were prepared under minimal light, and stored in the dark under nitrogen to prevent photo-oxidation. 9-Methylanthracene (9-MA) stock solutions, 0.02 M, were prepared using ethanol and also stored in the dark. Aliquots of 9-MA, 80 μl or less, were introduced to the CPZ samples contained in a 10-ml volumetric flask.

Care was taken to ensure all solutions contained the same volume of ethanol (0.8%). The dextrose stock solutions were prepared in buffer and added directly to the CPZ samples. All samples were stored in the dark and thermally equilibrated at the desired temperatures for 5 min before fluorescence experiments.

2.3. Fluorescence measurements

The fluorescence quencher molecule, 9-MA, was added incrementally to the CPZ solution and is assumed to reside exclusively within the micelle. Each MAN determination was carried out on seven solutions containing identical components except for increasing 9-MA concentrations, which range from 0.0 to 1.6×10^{-4} M. Samples were excited at 368 nm and emission intensities at 458 nm were used in all calculations. Fluorescence lifetime measurements were made using a scattering solution of glycogen as a reference with a 0.0-ns lifetime value. A 435-nm high-pass filter was used to block out the scattered excitation light. Cross-correlation frequency was set at 80 Hz, and scans were run at frequencies between 1 and 230 MHz. Data points were evaluated using a least-squares analysis on the phase and modulation data. All reported lifetime values were fitted to a χ^2 value of less than 7.5.

2.4. Differential scanning calorimetry

All DSC samples were prepared in a similar manner to those used in the fluorescence experiments. Samples were equilibrated at 20°C for 30 min before the first heating scan to 85°C and were subsequently cooled to 20°C. All temperature scans were carried out at a rate of 10°C/h. Consecutive duplicate heating and cooling scans were made on each sample. The reference solution contained phosphate buffer at the same concentration and pH as the samples. The thermograms were analyzed and the peak areas integrated using software provided by Calorimetry Sciences, Inc.

3. Results and discussion

3.1. Size of CPZ nanostructures as determined by fluorescence quenching

Using Poisson statistics to describe the distribution of 9-MA within the non-polar regions of the system, i.e. the interior of the CPZ nanostructures, and assuming that the CPZ micellar nanostructures will fluoresce fully only when unoccupied by a 9-MA molecule, the measured ratio of fluorescence intensities in the presence of 9-MA (I), to that in the absence of 9-MA (I^0), is obtained using Eq. (1)

$$(I^0/I) = \exp\{-[\text{9-MA}]/[M]\} \quad (1)$$

where $[M]$ is the micellar nanostructure concentration. For [CPZ] > cmc, Eq. (2) relates $[M]$ to the measurable concentration of CPZ, the cmc, and the MAN.

$$[M] = \frac{[\text{CPZ}] - \text{cmc}}{\text{MAN}} \quad (2)$$

The free monomer concentration in equilibrium with the micelles corresponds to the cmc. By combining Eqs. (1) and (2), the resulting Eq. (3) shown below provides the means to obtain the MAN value by plotting the values of ln (I^0/I) vs. [9-MA]:

$$\ln(I^0/I) = \frac{[\text{9-MA}](\text{MAN})}{[\text{CPZ}] - \text{cmc}} \quad (3)$$

All the cmc values used in this study were obtained by isothermal titration calorimetry in this laboratory [24], under similar experimental conditions.

The system used in our study fulfills the requirements set forth in Eq. (1). First, the quencher molecule is non-polar and associates exclusively with the lipophilic interior of the CPZ. Thus, quencher migration to the exterior of the micellar nanostructures effectively does not occur. The requirement of a Poissonian distribution of the quencher molecule in the system is also plausible

for systems involving relatively small organic molecules solubilized by micelles [25]. Second, the requirement for effective quenching is closely approximated by using excitation and emission wavelengths at 368 and 458 nm, respectively. This excitation wavelength is within the nanostructures' excitation range [8] and thus excitation of the monomer form of CPZ ($\lambda_{max} = 254.5$ nm [7]) is minimized. Next, monitoring the fluorescence intensity values at 458 nm allows for the greatest degree of quenching (see Fig. 1). Effective quenching of the occupied nanostructures is further supported by the observation that the fluorescence intensities at quencher concentrations higher than 1.6×10^{-4} M remained relatively constant. This may be due to saturation of the CPZ micellar nanostructures by quencher molecules in the system. Multiple 9-MA molecules may be present inside each micellar nanostructure resulting in a quenching saturation. Complete quenching of the system is not experimentally observed, probably due to the residual micelle fluorescence as well as emission from the monomers.

The steady-state fluorescence experiments yielded a MAN value of 37 ± 5 for a 10 mM CPZ in 0.1 M phosphate buffer (pH 6.5) at 25°C. Table 1 includes a list of previously reported aggregate sizes for CPZ under similar conditions. Only MAN values obtained using a specified concentration of ionic components were included for comparison. The agreement between our results and those of previous experiments indicates that the application of analyte fluorescence quenching without the use of an extrinsic probe molecule is appropriate for CPZ.

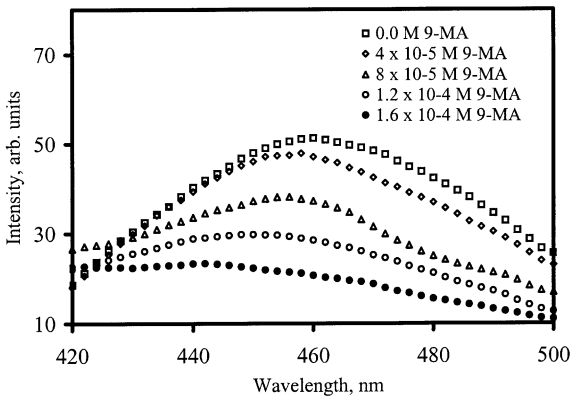

Fig. 1. A typical CPZ fluorescence quenching pattern with increasing 9-methylanthracene concentrations.

3.2. Effects of CPZ concentration

Although the cmc remains relatively constant as a function of CPZ concentration [8], the size of the micellar nanostructure does not. Fig. 2 illustrates the growth in MAN with increasing CPZ concentration. These results suggest an increase in the size of the nanostructures, supporting the step-wise aggregation theory of CPZ micelles [8]. Although the graph does not deconvolute the distribution of micelle sizes within the polydisperse system, it clearly shows that the average size of the nanostructures grows with the addition of CPZ monomers. Thus, while the free monomer concentration remains equal to the cmc, the CPZ nanostructures incorporate any additional monomers above the cmc to form larger aggregates.

The stabilization of CPZ micelles through $\pi-\pi$ stacking has been described by Attwood et al.

Table 1
Reference MAN values of CPZ in aqueous solution

[NaCl] mM	[CPZ] mM	MAN	Method	Reference
154	5.3	38	Gel filtration chromatography	Funasaki et al. [8]
154	4.6	35	Sedimentation equilibrium	Nichol et al. [20]
100	7.0	35	Light scattering	Attwood et al. [18]

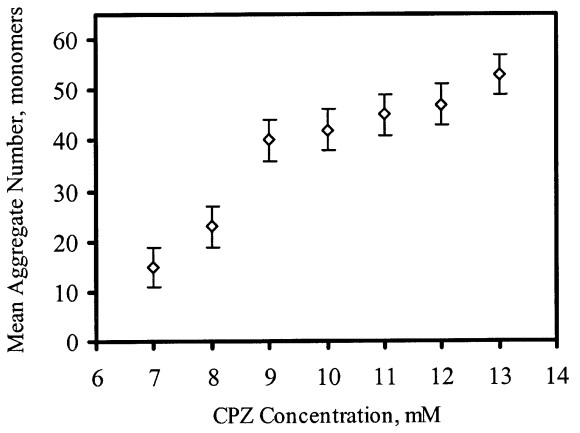

Fig. 2. Plot of the mean aggregate number vs. CPZ concentration in 0.1 M pH 6.5 phosphate buffer, 25°C.

[15]. These interactions lead to a stacking conformation, which supports the staircase model of the CPZ micelle [16]. The MAN is not a constant unit in equilibrium with monomers, but a dynamic quantity, which is highly dependent on the concentration of the drug above the cmc. Measurement of the aggregation values near the cmc (approx. 3 mM) was not possible using the fluorescence quenching technique. Furthermore, the MAN values at amphiphile concentrations higher than 13 mM were not measured due to the effects of CPZ fluorescence self-quenching at these concentrations.

3.3. Effects of osmolarity

Previous studies have reported an increase in the CPZ micelle size with increasing ionic strength of the system. This may be due to an increase in the hydrophobic effect [17]. A polar environment promotes unfavorable interactions between the aromatic moieties of CPZ and the solvent. Another reason for the increase in MAN with increasing NaCl concentration may be due to charge shielding by the chloride ions [19]. With increasing salt concentrations, a larger chloride ionic shell surrounds the positively charged, protonated amine groups, shielding their repulsive charge–charge interactions. We have extended these studies to include the effect of osmotic pressure on the size of the nanostructures by the addition of dextrose. Interactions of dextrose with CPZ are unlikely since CPZ favors ionic [26] and aromatic [13] interactions, neither of which is offered by dextrose. Protonation or deprotonation of the hydroxyl moieties of dextrose may be ruled out at the neutral pH of the system. The addition of dextrose is expected therefore to affect only the osmotic pressure of the system under the experimental conditions employed. We have determined the MAN values in CPZ solutions containing up to 0.3 M dextrose and found the MAN to remain relatively constant with increasing dextrose concentrations. Thus, increasing the osmotic pressure of the system has little effect on the micelle size. This leads to our conclusion that micellization of CPZ is affected by a change in the electrostatic conditions of the environment, and is not affected by osmotic pressure.

3.4. Effects of temperature

The thermodynamics of formation of micellar nanostructures are expected to be temperature dependent and should play a critical role in the aggregation process. With increasing temperatures (15–37°C), there may be a slight increase in the size of the nanostructures (see Fig. 3). This phenomenon is largely entropic in nature. The system's gain in entropy is achieved upon formation of the nanostructures and the subsequent release of water molecules from the hydration shells surrounding the monomers [9]. Yet, at elevated temperatures, the system shifts from an 'entropy-driven' one, to an 'enthalpy-driven' one. The size of the nanostructures decreases dramatically at temperatures higher than 37°C, and demicellization is achieved when 45°C is reached. This is marked by the precipitation of the quencher molecules, consistent with the general trend previously reported in other systems [27–29]. At higher temperatures the energy gain in the enthalpy of demicellization outweighs the effects of hydration shell entropy, to the point where the formation of the micellar nanostructures becomes unfavorable. With increasing temperature, there is a decrease in the unique ordered properties of water, which results in a more 'normal' polar fluid

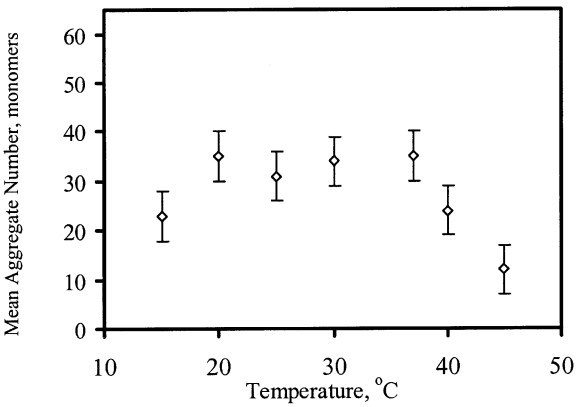

Fig. 3. Temperature dependence of the mean aggregate number for a 10 mM CPZ solution in phosphate buffer.

[30]. Thus the effects of hydrogen bonding between the solvent and the nanostructures become less significant, as do the unfavorable interactions between water molecules and the nonpolar moieties of the monomer. In addition, at higher temperatures, the positive entropy effect offered by the breakup of the micelles into monomers becomes significant. The strength of the counterion/monomer interactions also decreases [22]. The decrease in counterion binding will effectively lead to an increase in repulsive charge–charge interactions between adjacent monomers within the nanostructures. This will result in the increase of the repulsive forces and may contribute to a decrease in the size of the nanostructures and, ultimately, demicellization. Thus, changes in temperature have a profound effect on the MAN values.

3.5. The thermodynamics of micellization and demicellization

Direct measurements of the temperature and enthalpy of micellization and demicellization of nanostructures were recently reported by this laboratory [24] using differential scanning calorimetry. A linear increase in the temperature at which demicellization occurs was observed with increasing CPZ concentration (see Fig. 4). These results suggest a stabilization of the system at higher CPZ concentrations, in agreement with the stepwise increase in the mean aggregate number, supporting the fluorescence quenching results.

Interestingly, a similar trend was not observed for the enthalpy of demicellization (ΔH_{demic}) with increasing CPZ concentration. Fig. 5 illustrates the effect of CPZ concentration on the values of ΔH_{demic}. An initial increase in enthalpy with increasing CPZ concentration is indicative of a more stable system, which may be interpreted as an increase in the average micelle size. Yet, at higher CPZ concentrations, the ΔH_{demic} reaches a plateau of approximately 10 kJ/mol. This result seems to be an anomaly at first, given that the temperature at which demicellization occurs continues to increase. The explanation may lie in the polydispersity of the system. Although the average size of the micellar nanostructures may have increased at higher CPZ concentrations, the size distributions of aggregates may have changed resulting in certain shifts in dispersity. This may not be reflected in changes in the enthalpy values resulting in relatively constant ΔH_{demic} values at higher CPZ concentrations.

3.6. Fluorescence lifetime measurements

The CPZ fluorescence lifetimes were de-

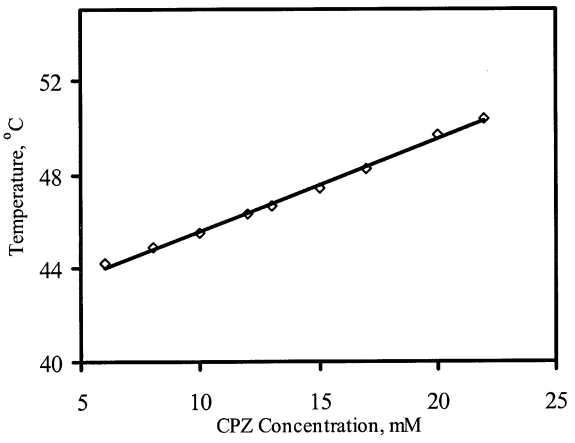

Fig. 4. Plot of the temperatures at which demicellization occurred as a function of increasing CPZ concentrations in 0.1 M pH 6.5 phosphate buffer.

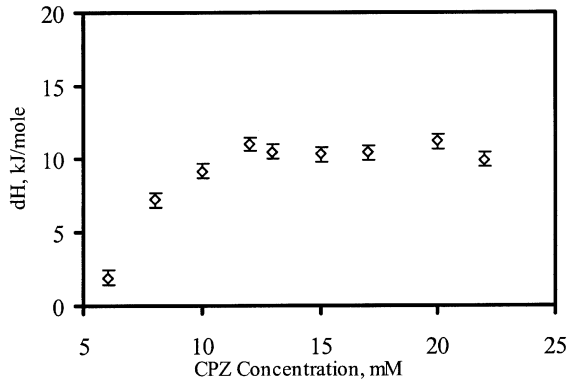

Fig. 5. Plot of the enthalpy change of demicellization with increasing CPZ concentration.

termined to provide additional insight into the polydispersity of the system. The results of the least-squares analysis for 10, 25 and 37°C are summarized in Tables 2–4, respectively, and showed that the lifetime values obtained at the different modulation frequencies were not consistent with a single component decay. The best fits to data obtained for CPZ concentrations below 4 mM were obtained by a two-component analysis, with two prevalent lifetime components. A shorter lifetime of no longer than 0.8 ns is present in all solutions of CPZ at pre- as well as post-cmc concentrations. This may be associated with those of lower order aggregates, i.e. monomers, dimers, and oligomers. These aggregates are less electronically stable relative to micelles, due to less $\pi-\pi$ stacking interactions. A second component with longer lifetimes ranging up to 6 ns becomes important at 3 mM and its contribution increases with higher CPZ concentrations. This may be assigned to the higher numbered CPZ aggregates, including micellar nanostructures. The CPZ micelles allow for more important $\pi-\pi$ interactions resulting in more delocalized and stable electronic interactions. Fig. 6 represents the average lifetime values of CPZ at 10°C taking into consideration the contributions of each lifetime to the entire system. The abrupt increase in the

Table 2
Results of the least-squares analysis on the CPZ decay at 10°C

[CPZ] mM	T_1, ns	f_1	T_2, ns	f_2	T_3, ns	f_3
1	0.6	0.91	5.9	0.09		
2	0.7	0.91	6.1	0.09		
3	0.7	0.83	4.6	0.17		
4	0.6	0.62	3.8	0.38		
5	0.8	0.29	3.8	0.61	1.4	0.11
6	0.8	0.26	3.7	0.61	1.3	0.13
10	0.8	0.23	3.7	0.57	1.4	0.20

T, lifetime; f, fractional intensity.

Table 3
Results of the least-squares analysis on the CPZ decay at 25°C

[CPZ] mM	T_1, ns	f_1	T_2, ns	f_2	T_3, ns	f_3
1	0.4	0.87	5.5	0.13		
2	0.5	0.89	5.8	0.11		
3	0.6	0.84	5.9	0.16		
4	0.5	0.40	3.7	0.52	1.7	0.08
5	0.8	0.32	4.1	0.48	1.7	0.20
6	0.7	0.26	3.2	0.51	1.6	0.23
10	0.7	0.18	3.1	0.56	1.5	0.26

T, lifetime; f, fractional intensity.

Table 4
Results of the least-squares analysis on the CPZ decay at 37°C

[CPZ] mM	T_1, ns	f_1	T_2, ns	f_2	T_3, ns	f_3
1	0.5	0.83	2.6	0.27		
2	0.5	0.81	2.9	0.29		
3	0.5	0.92	4.3	0.38		
4	0.6	0.41	3.8	0.51	1.7	0.08
5	0.6	0.30	3.0	0.50	1.7	0.20
6	0.6	0.16	2.7	0.54	1.6	0.30
10	0.6	0.12	2.4	0.56	1.5	0.32

T, lifetime; f, fractional intensity.

average lifetime values between 3 and 5 mM CPZ is an indication of the cmc. This is in excellent agreement with cmc values obtained in this laboratory using isothermal titration calorimetry [24]. Similar lifetime trends were observed at 25 and 37°C. The contribution from the shorter lifetime of not longer than 0.8 ns is dominant ($>80\%$) in pre-cmc concentrations of the amphiphile. This is compatible with the theory and experiments on CPZ micellization, which point toward a constant concentration of CPZ molecules not in micelle form above the cmc [8]. The contribution of the longer lifetime values is relatively small before the cmc, yet increases significantly to 60% upon formation of the nanostructure. This is consistent with micelle formation after the cmc. At concentrations above 12 mM CPZ, the data could not be fit accurately to single or multi-component lifetime values. This may be due to an additional increase in the dispersity of the system, which would support our constant enthalpy of demicellization results observed at higher concentrations of CPZ.

The CPZ fluorescence lifetimes were also determined with the addition of 9-MA up to 1.6×10^{-4} M to the CPZ solution. This caused no measurable change in the fluorescence lifetime decay of CPZ, confirming a static quenching mechanism by the incorporation of 9-MA into the micellar nanostructures.

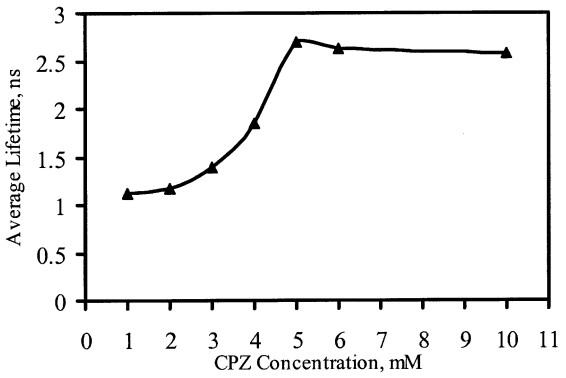

Fig. 6. The average fluorescence lifetimes for different CPZ concentrations in phosphate buffer at 10°C.

4. Conclusion

The mean aggregate number of CPZ nanostructures in solution was obtained using a modified version of the fluorescence quenching method by taking advantage of the native fluorescence of CPZ. The size of the CPZ micellar nanostructures is dependant on a number of parameters. With increasing CPZ concentration, the average size of the nanostructures increased in accordance to the step-wise aggregation theory. An increase in osmotic pressure, however, had no significant effect on the size of the nanostructures. The effects of temperature were significant at elevated temperatures, with demicellization occurring at approximately 45°C. The temperature at which demicellization occurs is concentration dependant, while the enthalpy of demicellization reaches a plateau at higher CPZ concentrations. This may be due to additional increases in the dispersity of the system, as evidenced by fluorescence lifetime measurements.

Acknowledgements

This work was supported by the Dreyfus Foundation, the Beckman Foundation, the Howard Hughes Medical Institute (HHMI) through the Undergraduate Biological Sciences Education Program, the American Chemical Society-Petroleum Research Fund, the NSF-REU program and Occidental College.

References

[1] E. Usdin, H. Eckert, I.S. Forrest, Elsevier, New York, Phenothiazines and Structurally Related Drugs: Basic and Clinical Studies, 7, 1979.
[2] P. Seeman, J. Weinstein, Erythrocyte membrane stabilization by tranquilizers and antihistamines, Biochem. Pharmacol. 15 (1966) 1737–1752.
[3] J.G. Elferink, Fluorescence studies of membrane interactions of chlorpromazine and chlorimipramine, Biochem. Pharmacol. 26 (1977) 511–515.
[4] D.E. Holmes, L.H. Piette, Effects of phenothiazine derivatives on biological membranes: drug-induced changes in electron spin resonance spectra from spin-labeled erythrocyte ghost membranes, J. Pharmacol. Exp. Ther. 173 (1970) 78–84.
[5] H.J. Muller, M. Luxnat, H.J. Galla, Lateral diffusion of small solutes and partition of amphipaths in defect structures of lipid bilayers, Biochim. Biophys. Acta 856 (1986) 283–289.
[6] T. Sato, O.S. Tsuyoshi, Effects of sulfhydryl reagents on the antisickling activity of some membrane-interacting compounds, Biochim. Biophys. Acta 727 (1983) 196–200.
[7] R. Welti, L.J. Mullikin, T. Yoshimura, G.M. Hlemkamp, Partition of amphiphilic molecules into phospholipid vesicles and human erythrocyte ghosts: measurements by ultraviolet difference spectroscopy, Biochemistry 23 (1984) 6086–6091.
[8] N. Funasaki, S. Hada, J. Paiement, Chromatographic study on the self-association of chlorpromazine hydrochloride in sodium chloride solution, J. Phys. Chem. 95 (1991) 4131–4135.
[9] S. Paula, W. Sues, J. Tuchtenhagen, A. Blume, Thermodynamics of micelle formation as a function of temperature: a high sensitivity titration calorimetry study, J. Phys. Chem 99 (1995) 11742–11751.
[10] E. Wajnberg, M. Tabak, P.A. Nussenzvieg, C.M.B. Lopes, S.R.W. Louro, pH-dependent phase transition of chlorpromazine micellar solutions in the physiological range, Biochim. Biophys. Acta 944 (1988) 185–190.
[11] N.D. Hinman, J.R. Cann, Reversible binding of chlorpromazine to brain tubulin, Mol. Pharmacol. 12 (1976) 769–777.
[12] M.J. Scully, L.W. Nichol, D.J. Winzor, Interactions between micellar ligand systems and acceptors: forms of binding curves, J. Theor. Biol. 90 (1981) 365–376.
[13] J.R. Cann, L.W. Nichol, D.J. Winzor, Micellarization of chlorpromazine. Implications in the binding of the drug to brain tubulin, Mol. Pharmacol. 20 (1981) 244–245.
[14] C. Tanford, The Hydrophobic Effect: Formation of Micelles and Biological Membranes, 2nd ed., John Wiley & Sons, New York, 1980.
[15] D. Attwood, R. Waigh, R. Blundell et al., ^{1}H and ^{13}C NMR studies of the self-association of chlorpromazine hydrochloride in aqueous solution, Mag. Res. Chem. 32 (1994) 472–486.
[16] P.K. Dea, H. Keyzer, Conformation and electronic aspects of chlorpromazine in solutionin: F. Gutman, H. Keyzer (Eds.), Modern Biochemistry, Plenum Press, New York, 1986.
[17] D. Attwood, R. Natarajan, Effect of pH on the micellar properties of amphiphilic drugs in aqueous solution, J. Pharm. Pharmacol. 33 (1981) 136–140.
[18] D. Attwood, R. Natarajan, Micellar properties of chlorpromazine hydrochloride in concentrated electrolyte solutions, J. Pharm. Pharmacol. 53 (1983) 317–319.
[19] V. Perez-Villar, M.E. Vazquez-Iglesias, A. de Geyer, Small-angle neutron scattering studies of chlorpromazine micelles in aqueous solutions, J. Phys. Chem. 97 (1993) 5149–5154.
[20] L.W. Nichol, E.A. Owen, D.J. Winzor, Quantitative characterization of micellar equilibria by sedimentation equilibrium. Micelle size and association constant for chlorpromazine, J. Phys. Chem. 86 (1982) 5015–5018.
[21] N.J. Turro, A. Yekta, Luminescent probes for detergent solutions. A simple procedure for determination of the mean aggregation number of micelles, J. Am. Chem. Soc. 100 (1978) 5951–5952.
[22] J. van Stam, S. Depaimelaere, F.C. De Schryver, Micellar aggregation numbers — A fluorescence study, J. Chem. Ed. 75 (1998) 93–97.
[23] M. Vasilescu, D. Angelescu, D.A.M. Almgren, A. Valstar, Interactions of globular proteins with surfactants studied with fluorescence probe methods, Langmuir 15 (1999) 2635–2643.
[24] Y.D. Saito, S. Tehrani, M.M. Okamoto, H.H. Chang, P. Dea, Calorimetry studies of chlorpromazine hydrochloride in solution, Langmuir 16 (2000) 6391–6395.
[25] M. Almgren, F. Grieser, J.K. Thomas, Energy transfer from triplet aromatic hydrocarbons to Tb^{3+} and Eu^{3+} in aqueous micellar solutions, J. Am. Chem. Soc. 101 (1979) 2021–2026.
[26] K.M. Markovich, T. Farooqui, L.J. Wallace, N.J. Uretsky, D.D. Miller, Enhancement of binding of quaternary ammonium derivatives of chlorpromazine to dopamine D-2 receptors by the addition of a H-bonding group, Bioorg. Med. Chem. Lett. 3 (1993) 1241–1244.
[27] M. Grubic, R. Strey, M. Teubner, On the application of

a laser T-jump apparatus for perturbation of ionic micellar solutions, J. Colloid Interface Sci. 80 (1981) 453–458.

[28] Y. Croonen, E. Gelade, M. Van der Zegel et al., Influence of salt, detergent concentration, and temperature on the fluorescence quenching of 1-methylpyrene in sodium dodecyl sulfate with *m*-dicyanobenzene, J. Phys. Chem. 87 (1983) 1426–1431.

[29] A. Malliaris, J. Le Moigne, J. Sturm, R. Zana, Temperature dependence of the micelle aggregation number and rate of intramicellar excimer formation in aqueous surfactant solutions, J. Phys. Chem. 89 (1985) 2709–2713.

[30] Y. Moroi, Micelles: Theoretical and Applied Aspects, Plenum Press, New York, 1992.